The Astrophysical Journal, 676:970–977, 2008 April 1

BLUE COMPACT DWARF GALAXIES WITH *SPITZER*: THE INFRARED/RADIO PROPERTIES

Yanling Wu,[1] V. Charmandaris,[2,3] J. R. Houck,[1] J. Bernard-Salas,[1] V. Lebouteiller,[1]
B. R. Brandl,[4] and D. Farrah[1]

Received 2007 August 1; accepted 2007 November 27

ABSTRACT

We study the correlation between the radio, mid-infrared, and far-infrared properties for a sample of 28 blue compact dwarf (BCD) and low-metallicity star-forming galaxies observed by *Spitzer*. We find that these sources extend the same far-infrared–to–radio correlation typical of star-forming late-type galaxies to lower luminosities. In BCDs, the 24 μm (or 22 μm) mid-infrared–to–radio correlation is similar to that of starburst galaxies, although there is somewhat larger dispersion in their q_{24} parameter compared to their $q_{\rm FIR}$. No strong correlations between the q parameter and galaxy metallicity or effective dust temperature have been detected, although there is a hint of decreasing q_{24} at low metallicities. The two lowest metallicity dwarfs in our sample, I Zw 18 and SBS 0335−052E, despite their similar chemical abundance, deviate from the average q_{24} ratio in opposite manners, displaying an apparent radio excess and dust excess, respectively.

Subject headings: galaxies: dwarf — galaxies: starburst — infrared: galaxies — radio continuum: galaxies

1. INTRODUCTION

More than 35 years ago, a correlation between the 10 μm mid-infrared (mid-IR) and 1.4 GHz luminosities in galactic nuclei was first noticed by van der Kruit (1971). In 1983, the launch of the *Infrared Astronomical Satellite (IRAS)* brought a new era in collecting large samples of data in the infrared and sparked numerous studies investigating the above-mentioned correlation in star-forming galaxies. Both the radio and infrared emission are closely related to star formation activities. The radio continuum is known to originate from two processes: thermal free-free emission from ionized gas in H II regions and nonthermal synchrotron radiation from relativistic electrons that are accelerated in the supernova remnants (SNRs; see Condon 1992 for a review). The thermal emission usually has a rather flat spectrum with $f_\nu \propto \nu^{-0.1}$, while the nonthermal component often has a much steeper spectral slope with $f_\nu \propto \nu^{-0.8}$. In normal galaxies the relative contribution of the two components varies with frequency and at 1.4 GHz the radio continuum is dominated (at nearly ~90%) by the nonthermal component. The infrared emission is due to the thermal reradiation of starlight from dust surrounding H II regions (Harwit & Pacini 1975). Based mostly on *IRAS* data, it has been shown that the far-infrared (FIR; 40–120 μm) to radio correlation holds well over a remarkably wide range of star-forming galaxies, spanning several orders of magnitude in luminosity (Helou et al. 1985; de Jong et al. 1985; Condon et al. 1991; Yun et al. 2001). The availability of deep observations of distant galaxies by the *Infrared Space Observatory* (*ISO*) and recently by *Spitzer* (Werner et al. 2004) showed that the correlation between the IR and radio emission is not limited to the local universe but also extends to galaxies at higher redshifts (Garrett 2002; Appleton et al. 2004). It was also revealed that in addition to the FIR, the mid-IR emission at ~24 μm correlates with the 20 cm radio continuum, although with more scatter (Elbaz et al. 2002; Gruppioni et al. 2003; Appleton et al. 2004; Wu et al. 2005). A number of very deep *Spitzer* mid-IR and FIR surveys can now probe a population of galaxies with low-infrared luminosities for which ancillary data, including deep radio imaging, are becoming available (e.g., Jannuzi & Dey 1999; Sanders et al. 2008; Rosenberg et al. 2006). This is particularly interesting, since in the near future ~20 μm is the longest wavelength that will likely be probed by the *James Webb Space Telescope*. It is thus instructive to examine the mid-IR–to–radio correlation in more detail in these low-luminosity nearby systems, for which little is known to date.

As ubiquitous as the FIR/radio correlation appears to be, there are a few significant deviations from it. Radio excess exists in some instances, such as galaxies hosting an active galactic nucleus (AGN). External magnetic field compression due to the interaction with nearby galaxies could also produce extra emission in the radio continuum (Miller & Owen 2001). Conversely, synchrotron deficiency has been found in some nascent starburst galaxies studied by Roussel et al. (2003, 2006), which was attributed to the lack of time for massive young stars to evolve into supernovae (SN) since these galaxies are just at the onset of a starburst episode. On the other hand, in the infrared, dust emission can be damped in an optically thin environment, because the ultraviolet (UV) and optical light may not be fully reprocessed by the dust, as seen in low-luminosity dwarf galaxies.

Blue compact dwarf galaxies are a group of extragalactic objects that are characterized by their blue optical colors, small sizes ($\leq$1 kpc), and low luminosities ($M_B > -18$). These galaxies do not display any AGN signature[5] and have recent bursts of star formation in a relatively unevolved chemical environment. As such they have been proposed as nearby analogs of star formation in young galaxies in the early universe. In a metal-poor environment, star-forming regions are usually optically thin and emit less in the infrared. However, Devereux & Eales (1989) suggested that in a low-luminosity galaxy, the radio emission also decreases, and probably faster than the infrared. The deficiencies in both the nonthermal radio and FIR emission may counterbalance each other and result in a similar FIR/radio ratio to that observed in normal spiral galaxies (Klein et al. 1991). This was examined by a study of

[1] Astronomy Department, Cornell University, Ithaca, NY 14853.
[2] Department of Physics, University of Crete, GR-71003 Heraklion, Greece.
[3] IESL/Foundation for Research and Technology-Hellas, GR-71110 Heraklion, Greece and Chercheur Associé, Observatoire de Paris, F-75014 Paris, France.
[4] Leiden Observatory, Leiden University, P.O. Box 9513, 2300 RA Leiden, Netherlands.

[5] A possible exception among our sources is CG0752 in which the high ionization lines [Ne v] λ14.3/24.3 μm are detected (see L. Hao et al. 2008, in preparation).

star formation rates (SFRs) in BCDs performed by Hopkins et al. (2002) in which the authors found an excellent agreement between the SFRs estimated from 1.4 GHz and 60 μm luminosities. As Bell (2003) has pointed out, however, the FIR/radio correlation is almost linear, not because the IR and radio emission reflect the SFRs correctly but because in low-luminosity galaxies they are both underestimated by similar factors. This is in agreement with Helou & Bicay (1993) who found from their modeling work in disk galaxies that the transparency of the disk was about the same to both reemission processes. Hunt et al. (2005a) in their analysis of the spectral energy distributions (SEDs) of low-metallicity BCDs noticed that these systems do not follow several of the usual correlations between the mid-IR, FIR, and radio emission and display a scatter of a factor of $\sim$10.

The *Spitzer Space Telescope* has enabled us to study the infrared properties of a large sample of BCDs, probing the lower end of the luminosity and metallicity range. In this paper, the fifth in a series (Houck et al. 2004b; Wu et al. 2006, 2007, 2008), we examine their mid-IR– and FIR-to-radio correlation, extending the work of Hopkins et al. (2002). We describe the sample selection and the observational data in § 2. A detailed study of mid-IR and FIR/radio correlation, as well as its dependence with other parameters, such as metallicity and dust temperature, is presented in § 3. We also discuss two extreme cases, I Zw 18 and SBS 0335−052, in § 3. We summarize our conclusions in § 4.

2. OBSERVATIONS

As part of the IRS[6] (Houck et al. 2004a) Guaranteed Time Observation (GTO) program (PID: 85), we have compiled a sample of BCD candidates ($\sim$64) selected from the Second Byurakan Survey (SBS), Bootes void galaxies (Kirshner et al. 1981; Popescu & Hopp 2000), and other commonly studied BCDs. These sources are known to have low metallicities ranging from 0.03 to 0.5 $Z_{\odot}$.[7] Their 22 μm fluxes have been published in Wu et al. (2006). We also include 10 galaxies from Engelbracht et al. (2005; PID: 59), which are mostly BCDs and starburst galaxies and span a larger metallicity range (0.03−1.5 $Z_{\odot}$).[8] For all galaxies with 22 (24) μm detections, we searched the literature, as well as the public archives (NVSS and FIRST), for 1.4 GHz radio continuum data. We restrict our sample to sources with both mid-IR and radio detections, which results in a sample of 23 galaxies. Finally, we also include 5 galaxies that have 22 μm detections and 1.4 GHz upper limits published by Hopkins et al. (2002) for comparison between our and Hopkins' samples. Note that the sample was not selected based on infrared properties, but merely on BCD-type objects and the availability of both infrared and radio data. As a result, our sample is not complete, but the large number of sources that only became detectable in the infrared with *Spitzer* allows us to probe the properties of low-luminosity dwarf galaxies and provide statistically meaningful results. The observational information for this sample and previously published data are presented in Table 1, which includes the positions of the sources and their mid-IR, FIR, and 1.4 GHz flux densities, as well as oxygen abundances of the ionized gas.

All sources in this study have mid-IR flux measurements either at 22 μm with the IRS red peak-up camera and/or at 24 μm with MIPS (Rieke et al. 2004). The photometric fluxes of these two bands differ by less than 10% for galaxies in the local universe. This was confirmed by using a suite of $\sim$100 spectra of nearby galaxies from our IRS/GTO database and calculating their synthetic 22 and 24 μm fluxes after convolving the spectra with the corresponding filter response curves. For consistency, in our analysis we use the MIPS 24 μm measurements, and the 22 μm values are only used when the 24 μm values are not available. For sources above the IRS 22 μm and MIPS 24 μm saturation limits we use the IRS low-resolution spectrum to estimate a synthetic 24 μm flux. We also obtained far-infrared fluxes for our sample from the archival *IRAS* 60 and 100 μm data (Moshir & et al. 1990; Sanders et al. 2003).

Most of the 1.4 GHz radio continuum data are from the NRAO VLA Sky Survey (NVSS; Condon et al. 1998), while one is from Faint Images of the Radio Sky at Twenty cm (FIRST; Becker et al. 1995), along with some individual observations (references in Table 1). A total of seven sources were too faint and were not included in the NVSS catalog. For those we used the values of Hopkins et al. (2002), who studied a similar BCD sample and remeasured the 1.4 GHz fluxes using the images from NVSS and FIRST, providing radio detections for two sources and better upper limits for another five sources that overlap with the galaxies in our sample.

Our final sample consists of 28 galaxies, all of which have *Spitzer* mid-IR 24 μm and/or 22 μm flux measurements. Among these galaxies, 23 sources have 1.4 GHz radio continuum data and five have measured upper limits. *IRAS* 60 and 100 μm fluxes are available for 16 sources, and 3 more are detected only at 60 μm. We list the photometry of our sources in Table 1. The uncertainty in the 22 or 24 μm photometry is less than 5%. The *IRAS* 60 and 100 μm fluxes typically have less than a few percent of error but could go up to $\sim$15% for some of the fainter sources. The rms noise level for NVSS is $\sim$0.5 mJy beam^{-1}.

3. RESULTS

3.1. *Mid-IR– and FIR-to-Radio Correlation in BCDs*

The sensitivity and efficiency of the *Spitzer Space Telescope* have allowed us to probe the correlation between the mid-IR and radio luminosities for a large number of galaxies. Using the 24 and 70 μm MIPS imaging data of the First Look Survey, Appleton et al. (2004) have demonstrated the first direct evidence for the universality of the mid-IR/radio and FIR/radio correlation to $z \sim 1$. Wu et al. (2005) have also studied the mid-IR/radio correlation in a sample of star-forming galaxies and found that both the 8 and 24 μm luminosity are clearly correlated with the 1.4 GHz radio luminosity. Their sample included only a few (three) dwarf galaxies and suggested that there may be a slope change for dwarf galaxies, which could be due to the lower dust-to-gas ratios and lower metallicities of the dwarfs. A detailed analysis of the spatial distribution of the infrared-to-radio correlation using *Spitzer* data on a sample of nearby late-type spiral galaxies has been performed by Murphy et al. (2006a, 2006b) in which the authors found that the ratio of the mid-IR and FIR to radio emission does vary from one region to the other. In general, however, the dispersion is small and the ratio decreases with surface brightness and galactocentric radius.

Using the data from this sample of low-metallicity dwarf galaxies we plot in Figure 1 the radio luminosity of the sample as a

[6] The IRS was a collaborative venture between Cornell University and Ball Aerospace Corporation funded by NASA through the Jet Propulsion Laboratory and the Ames Research Center.

[7] Here we adopt the new oxygen solar abundance of $12 + \log(\mathrm{O/H}) = 8.69$ (Allende Prieto et al. 2001). Wu et al. (2008) have derived neon and sulfur abundances for a sample of BCDs using the infrared data, but these abundances are not available for all of the sources in this study.

[8] The galaxies in PID 59 partly overlap with the BCDs in PID 85. We have also excluded some galaxies from which the authors derived their 24 μm fluxes by doing a color correction to the *IRAS* 25 μm fluxes because of the aperture difference between these two band filters.

TABLE 1
PROPERTIES OF THE SAMPLE

ID	Object Name	R.A. J2000	Decl. J2000	Flux (mJy) 1.4 GHz	24(22) μm	60 μm	100 μm	$12 + \log(O/H)$	References 1.4 GHz	24 μm	*IRAS*	*Z*
1.....	Haro 11	00 36 52.5	−33 33 19	26.8	1900	6880	5040	7.9	1	2	3	4
2.....	NGC 1140	02 54 33.6	−10 01 40	23.6	316.6	3358	4922	8.5	1	5	6	7
3.....	SBS 0335−052E	03 37 44.0	−05 02 40	0.46	66	...	...	7.3	8	2	...	9
4.....	NGC 1569	04 30 47.0	+64 50 59	336.3	2991	54360	55290	8.2	1	2	3	10
5.....	II Zw 40	05 55 42.6	+03 23 32	32.5	1500	6570	5270	8.1	1	2	3	7
6.....	UGC 4274	08 13 13.0	+45 59 39	10.5	240	3236	6448	8.5	1	2	6	...
7.....	He 2-10	08 36 15.2	−26 24 34	83.8	4900	...	...	8.9	1	2	...	11
8.....	NGC 2782	09 14 05.1	+40 06 49	124.5	960	9170	13760	8.8	1	2	3	12
9.....	NGC 2903	09 32 10.1	+21 30 03	444.5	2200	60540	130430	9.3	1	2	3	11
10.....	I Zw 18	09 34 02.0	+55 14 28	1.83	5.5	...	...	7.2	13	2	...	9
11.....	SBS 0940+544	09 44 16.7	+54 11 33	<2.3	2.3	...	...	7.5	14	5	...	15
12.....	NGC 3077	10 03 19.1	+68 44 02	29.0	1500	15900	26530	8.6	1	2	3	16
13.....	Mrk 153	10 49 05.0	+52 20 08	4.0	29	280	<480	7.8	1	2	6	17
14.....	VII Zw 403	11 27 59.9	+78 59 39	1.2	28	...	...	7.7	18	2	...	9
15.....	Mrk 1450	11 38 35.6	+57 52 27	<2.0	48	279	<575	8.0	14	2	6	7
16.....	UM 448	11 42 12.4	+00 20 03	32.6	560	4139	4321	8.0	1	2	6	7
17.....	UM 461	11 51 33.3	−02 22 22	<2.6	30	...	...	7.8	14	2	...	9
18.....	UM 462	11 52 37.3	−02 28 10	5.8	110	944	896	8.0	1	2	6	9
19.....	SBS 1159+545	12 02 02.4	+54 15 50	<2.3	6.4	...	...	7.5	14	5	...	19
20.....	NGC 4194	12 14 09.5	+54 31 37	100.7	3100	23200	25160	8.8	1	2	3	16
21.....	NGC 4670	12 45 17.1	+27 07 32	13.7	210	2634	4470	8.2	1	2	6	12
22.....	SBS 1415+437	14 17 01.4	+43 30 05	4.3	19.6	...	...	7.6	14	5	...	9
23.....	Mrk 475	14 39 05.4	+36 48 21	<2.7	10.8	...	...	7.9	14	5	...	9
24.....	CG 0563	14 52 05.7	+38 10 59	6.2	97.0	870	1900	8.7	1	...	6	...
25.....	CG 0752	15 31 21.3	+47 01 24	4.8	138.9	837	1059	...	1	5	6	...
26.....	SBS 1533+574	15 34 13.8	+57 17 06	4.2	53.4	257	405	8.1	14	5	6	9
27.....	Mrk 1499	16 35 21.1	+52 12 53	1.5	33.8	256	617	8.1	20	5	6	21
28.....	Mrk 930	23 31 58.3	+28 56 50	12.2	170	1245	<2154	8.1	1	2	6	7

NOTE.—Units of right ascension are hours, minutes, and seconds, and units of declination are degrees, arcminutes, and arcseconds.
REFERENCES.—(1) Condon et al. 1998; (2) Engelbracht et al. 2005; (3) Sanders et al. 2003; (4) Bergvall & Östlin 2002; (5) Wu et al. 2006; (6) Moshir et al. 1990; (7) Guseva et al. 2000; (8) Hunt et al. 2004; (9) Izotov & Thuan 1999; (10) Kobulnicky & Skillman 1997; (11) Kobulnicky & Johnson 1999; (12) Heckman et al. 1998; (13) Hunt et al. 2005b; (14) Hopkins et al. 2002; (15) Thuan & Izotov 2005; (16) Storchi-Bergmann et al. 1994; (17) Kunth & Joubert 1985; (18) Leroy et al. 2005; (19) Izotov & Thuan 1998; (20) FIRST catalog; (21) Shi et al. 2005.

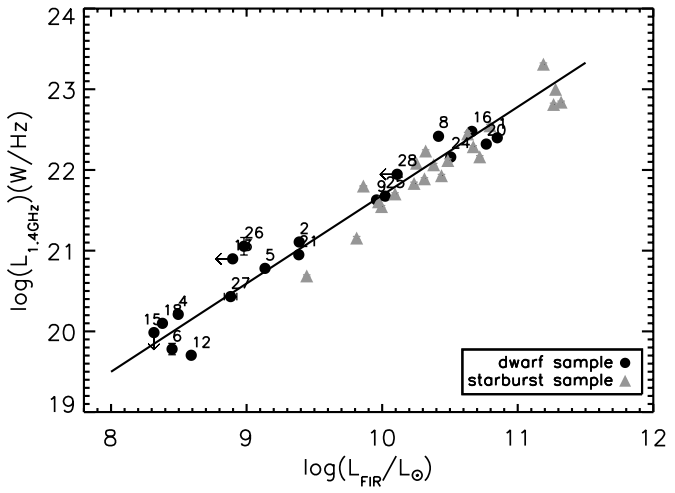

FIG. 1.—FIR to 1.4 GHz radio luminosity correlation for this sample. Our data are presented with filled circles. The numbers next to each symbol correspond to their IDs in Table 1. The solid line shows the best fit to this sample excluding the upper limits. For comparison, we have also included the starburst galaxies of Brandl et al. (2006; *triangles*).

function of the FIR luminosity. The luminosities of the sources that we study span nearly 4 orders of magnitudes but the correlation between the FIR and the radio is remarkably tight. The scatter in the ratio of the FIR and radio luminosities is 0.23 dex, i.e., less than a factor of 2. We performed a least-squares bisector fit to the data and found: $\log[L_{1.4\,\mathrm{GHz}}(\mathrm{W\ Hz^{-1}})] = 1.09\log(L_{\mathrm{FIR}}/L_{\odot}) + 10.75$. For comparison, we have included in the plot the starburst galaxies from Brandl et al. (2006) marked with triangles, which have an identical slope (within 1 σ). This slope of 1.09 ± 0.07 for the dwarf galaxy data agrees well with the slope of 1.10 ± 0.04 found by Bell (2003) for a sample of 162 galaxies, as well as the slope of 1.11 ± 0.02 for the infrared-selected sources from the *IRAS* Bright Galaxy Sample (BGS; Condon et al. 1991). This is also in agreement with Hopkins et al. (2002) and would suggest that globally our BCDs have a very similar FIR/radio correlation to that of normal galaxies.

Another way to parameterize the IR/radio correlation is to calculate the ratio of FIR to radio luminosity q_{FIR} according to the Helou et al. (1985) formula, as well as the q_{24} following the definition of Appleton et al. (2004).[9] We plot the q_{24} values for our sample as a function of the 24 μm luminosity of the galaxies in

[9] We use $q_{\mathrm{FIR}} = \log[1.26\times10^{-14}(2.58S_{60\,\mu\mathrm{m}} + S_{100\,\mu\mathrm{m}})/(3.75\times10^{12}F_{1.4\,\mathrm{GHz}})]$, where $S_{60\,\mu\mathrm{m}}$ and $S_{100\,\mu\mathrm{m}}$ are in Jy and $F_{1.4\,\mathrm{GHz}}$ is in $\mathrm{Wm^{-2}\,Hz^{-1}}$ (Helou et al. 1985). We also define $q_{24} = \log(S_{24\,\mu\mathrm{m}}/S_{1.4\,\mathrm{GHz}})$, where $S_{24\,\mu\mathrm{m}}$ and $S_{1.4\,\mathrm{GHz}}$ are in Jy as in Appleton et al. (2004).

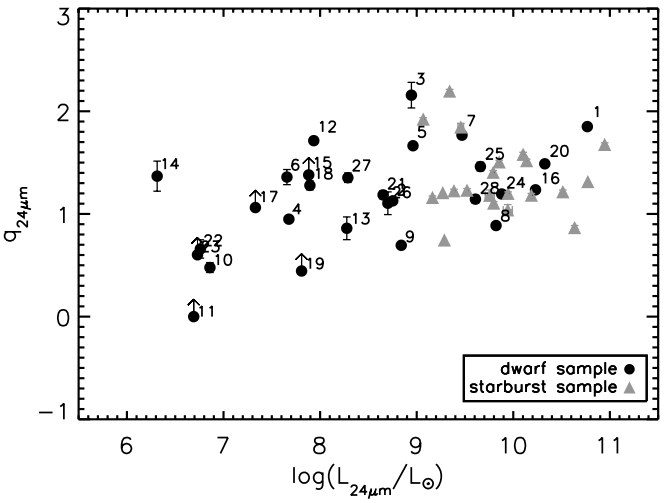

FIG. 2.—Plot of q_{24} as a function of the 24 μm monochromatic luminosity L_{24}. The symbols are the same as in Fig. 1.

Figure 2. For this sample we find that $q_{\rm FIR} = 2.4 \pm 0.2$, consistent with the value of normal galaxies of $q_{\rm FIR} = 2.3 \pm 0.2$ found by Condon (1992). When using the mid-IR 24 μm data, we find that $q_{24} = 1.3 \pm 0.4$ (see Table 2). The standard deviation in q_{24} is roughly twice that of $q_{\rm FIR}$. This is not unexpected given that the spectrum of star-forming galaxies shows substantially larger variations in spectral slope in the mid-IR (see Brandl et al. 2006) than in the FIR (Dale et al. 2006). A small change in the geometry of the emitting regions would affect $F_\nu(24\ \mu{\rm m})$ and thus the q_{24} ratio much more than the FIR emission and $q_{\rm FIR}$. A similar result has also been noticed by Appleton et al. (2004) and Murphy et al. (2006a), who found a larger dispersion in q_{24} as compared to q_{70}[10] and suggested that this is probably due to a larger intrinsic dispersion in the IR/radio correlation at shorter wavelengths. Interestingly, the Appleton et al. (2004) values for $q_{24} = 0.84 \pm 0.28$ or the k-corrected q_{24} of 0.94 ± 0.23 are somewhat smaller than our results, although consistent within 2 σ. One possible explanation is that the dust temperature of low-luminosity dwarf galaxies tends to peak at shorter wavelength than normal star-forming galaxies, which would result in an elevated 24 μm–based luminosity. An alternative explanation is that due to the peculiar morphology of dwarf galaxies, more electrons escape from the galaxy because of the cosmic-ray diffusion. Boyle et al. (2007) have also found a high $q_{24} = 1.39 \pm 0.02$ for the sources that they studied, and they postulated that this may be due to a change in the mean q_{24} ratio for objects with $F_\nu(24\ \mu{\rm m}) < 1$ mJy; however, their sources are much farther away and may not be comparable to the low-metallicity star-forming galaxies that we study in the local universe.

3.2. *Metallicity and Dust Temperature Effects on* $q_{\rm IR}$

A number of physical parameters, such as the metallicity, dust grain size distribution, and temperature, may affect the shape of the

[10] We define $q_{70} = \log(S_{70\ \mu{\rm m}}/S_{1.4\ {\rm GHz}})$, where $S_{70\ \mu{\rm m}}$ and $S_{1.4\ {\rm GHz}}$ are in Jy as in Appleton et al. (2004).

TABLE 2
DERIVED QUANTITIES OF THE SAMPLE

ID	Object Name	Distance[a] (Mpc)	$L_{1.4\ {\rm GHz}}$ ($\times 10^{20}$ W Hz^{-1})	$L_{24\ \mu{\rm m}}$ ($\times 10^8\ L_\odot$)	$L_{\rm FIR}$ ($\times 10^8\ L_\odot$)	q_{24}	$q_{\rm FIR}$
1.....	Haro 11	88	250.5	584.2	706.3	1.85	2.46
2.....	NGC 1140	21.2	12.8	5.6	24.4	1.13	2.29
3.....	SBS 0335−052E	58	18.7	8.8	...	2.16	...
4.....	NGC 1569	2.0	1.6	0.5	3.1	0.95	2.29
5.....	II Zw 40	12.4	6.0	9.2	13.7	1.66	2.36
6.....	UGC 4274	6.9	0.6	0.5	2.8	1.36	2.68
7.....	He 2-10	12	15.6	29.9	...	1.77	...
8.....	NGC 2782	41.7	216.3	66.3	260.4	0.89	2.00
9.....	NGC 2903	8.9	42.5	6.9	90.9	0.69	2.34
10.....	I Zw 18	18.2	0.7	0.07	...	0.48	1.31[b]
11.....	SBS 0940+544	23	< 1.5	0.05	...	>0.00	...
12.....	NGC 3077	3.8	0.5	0.9	3.9	1.71	2.89
13.....	Mrk 153	40.5	7.9	1.9	<7.9	0.86	<2.00
14.....	VII Zw 403	4.3	0.03	0.02	...	1.37	...
15.....	Mrk 1450	20.0	<1.0	0.8	<2.1	>1.38	...
16.....	UM 448	87.4	300.6	188.9	458.6	1.23	2.19
17.....	UM 461	13.4	<0.6	0.2	...	>1.06	...
18.....	UM 462	13.4	1.3	0.8	2.4	1.28	2.29
19.....	SBS 1159+545	50	<7.0	0.6	...	>0.44	...
20.....	NGC 4194	41.5	209.3	212.0	586.0	1.49	2.45
21.....	NGC 4670	23.2	8.9	4.5	24.3	1.19	2.44
22.....	SBS 1415+437	8.7	0.4	0.06	...	0.66	...
23.....	Mrk 475	11.2	<0.4	0.05	...	>0.60	...
24.....	CG 0563	139	144.6	74.4	320.5	1.19	2.35
25.....	CG 0752	90	47.3	45.1	105.3	1.46	2.35
26.....	SBS 1533+574	47	11.3	4.7	9.6	1.10	1.93
27.....	Mrk 1499	39	2.7	2.0	7.6	1.35	2.46
28.....	Mrk 930	77.5	88.4	40.5	<129.0	1.14	<2.17

[a] The distances to the galaxies of the sample are adopted from Moustakas & Kennicutt (2006) when available, while the rest of the sources are calculated from the redshifts taken from NED, assuming a ΛCDM cosmology with $H_0 = 70$ km s^{-1} Mpc^{-1}, $\Omega_m = 0.3$, and $\Omega_\lambda = 0.7$. For I Zw 18, we adopt the newly derived distance by Aloisi et al. (2007). The average uncertainty in the distances is ~5%, mainly due to the value of H_0.

[b] This is calculated based on the "equivalent" *IRAS* 60 and 100 μm fluxes (see § 3.4).

infrared SED. Consequently, we search for correlations between the q ratios of the galaxies in our sample with those parameters. Our sample covers a metallicity range of $7.2 \leq 12 + \log(\mathrm{O/H}) \leq 8.9$. In low-metallicity galaxies, the dust content is usually low, even though there are notable exceptions such as SBS 0335−052E (Houck et al. 2004b); thus, the emission of UV light might not be fully reprocessed by the dust and reemitted at the infrared wavelengths. However, these galaxies might have a quenched synchrotron radiation. This can be attributed to various reasons, including a lack of supernova remnants that accelerate particles producing radio emission, the escape of fast cosmic rays from the galaxy, etc. These two competing factors, dust and radio emission, counterbalance each other (see Bell 2003). BCDs, however, are typically small, less than ∼1 kpc in size, and have fewer H II regions with massive stars (with regard to normal galaxies) that heat the dust and go supernova to produce cosmic rays. As a result, the averaging effects in the sampling of the properties of the interstellar medium that result from the limited spatial resolution in dense galactic disks are not so prominent in BCDs. Furthermore, the small number of statistics may also contribute to the observed higher dispersion in q_{24} ratios in metal-poor dwarf galaxies. We investigate how metallicity affects the q_{24} ratios by dividing the dwarf galaxies in our sample into two groups: a lower metallicity group with $12 + \log(\mathrm{O/H}) \leq 8.0$ and a higher metallicity group with $12 + \log(\mathrm{O/H}) > 8.0$. This metallicity threshold was selected following Rosenberg et al. (2008), who noticed a change in the properties of the star-forming dwarf galaxies that they studied around this metallicity value. We find a mean $q_{24} = 1.1 \pm 0.1$[11] for the first group and $q_{24} = 1.3 \pm 0.1$ for the second one. If we calculate the q_{24} for the low-metallicity group without including SBS 0335−052E, we find a much lower $q_{24} = 0.9 \pm 0.1$.

We also notice that it appears that q_{24} generally decreases with reduced metallicity for sources with $12 + \log(\mathrm{O/H}) < 8.0$, with SBS 035−052E as a clear outlier, and the slope flattens out at $12 + \log(\mathrm{O/H}) > 8.0$ (see Fig. 3). This scatter in q_{24} at higher metallicities could be attributed to the greater dispersion in the mid-IR emission in these sources and is consistent with a number of other studies that have found increased dispersion in the q ratios for very high luminosity galaxies (which usually have higher metallicities; Condon et al. 1991; Yun et al. 2001; Bell 2003).

Hummel et al. (1988) have found evidence that, for a given galaxy, there is a small decrease in $F(100\ \mu\mathrm{m})/S(20\ \mathrm{cm})$ when the dust temperature increases. The latter can be traced by the ratio of $F(60\ \mu\mathrm{m})/F(100\ \mu\mathrm{m})$. Roussel et al. (2003) reached a similar result for the starburst galaxies that they studied, in which they detected an anticorrelation of q_{FIR} with $F(60\ \mu\mathrm{m})/F(100\ \mu\mathrm{m})$. However, performing the same test for the q_{24} ratios on our dwarf galaxy sample that spans a range of flux ratios $-0.4 < \log[F(60\ \mu\mathrm{m})/F(100\ \mu\mathrm{m})] < 0.2$ we find no such clear trend. It is conceivable that this is partly because our sample is too small to identify a trend due to the intrinsic scatter in q_{24}.

3.3. *Star Formation Rate Estimates*

Both the radio and infrared emission can be used to estimate the SFRs in galaxies. However, these correlations depend on a number of parameters including dust content, optical depth, and metallicity. This topic and potential caveats have been discussed extensively in the literature (see Condon 1992; Kennicutt 1998 and references therein). For dwarf galaxies, the topic has been addressed in detail by Hopkins et al. (2002). The recent wealth of data from *Spitzer* has also provided sufficient motivation to establish a calibration for the SFR using the infrared. Wu et al. (2005) and more recently Calzetti et al. (2007) have explored this topic using a large sample of star-forming regions and nearby galaxies.

[11] Here we use the standard error of the mean (SEM) to quantify the dispersion in the mean value.

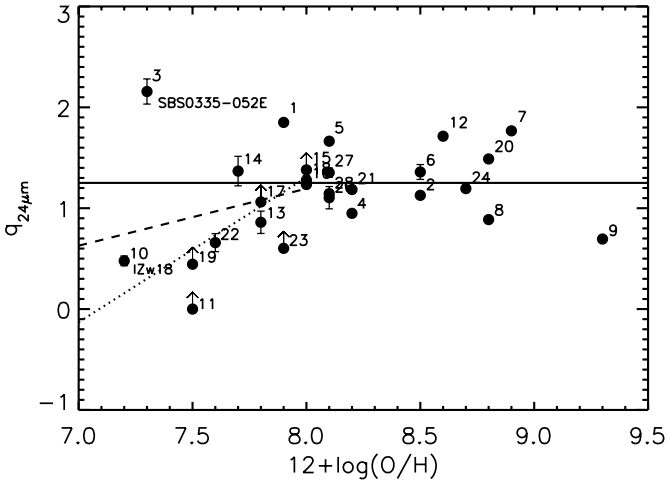

FIG. 3.—The q_{24} ratio plotted as a function of the oxygen abundance of the BCDs. The mean q_{24} value for all the sources is indicated by the solid line. A fit to the low-metallicity sources $[12 + \log(\mathrm{O/H}) \leq 8.0]$ is indicated by the dashed line, while the dotted line is the same fit excluding SBS 0335−052E.

In Figure 4 we plot the IR estimated SFR for our sample using the calibrations proposed by Wu et al. (2005) and Calzetti et al. (2007), respectively:

$$\mathrm{SFR}_{24}\left(M_\odot\ \mathrm{yr}^{-1}\right) = \frac{\nu L_\nu(24\ \mu\mathrm{m})}{6.66\times10^8\ L_\odot}, \quad (1)$$

$$\mathrm{SFR}_{24}\left(M_\odot\ \mathrm{yr}^{-1}\right) = 1.27\times10^{-38}\left[L_{24}\left(\mathrm{ergs}^{-1}\right)\right]^{0.885} \quad (2)$$

as a function of the well-known radio-to-SFR formula of Condon (1992):

$$\mathrm{SFR}_{1.4\ \mathrm{GHz}} = 5.5\times\frac{L_{1.4\ \mathrm{GHz}}}{4.6\times10^{21}\ \mathrm{W\ Hz}^{-1}}. \quad (3)$$

The Wu et al. (2005) work is based on a global correlation without separating the low-metallicity sources from metal-rich galaxies. As can be seen in Figure 4, a good agreement exists between the radio and IR estimated SFRs (indicated by diamonds). If we use the more recent calibration by Calzetti et al. (2007) on SFRs from 24 μm luminosities, we find that most of the mid-IR estimated SFRs (*filled circles*) are located below the 1 : 1 proportionality line, and thus they are consistently lower than both the SFRs estimated from the radio or from Wu et al. (2005). This is not unexpected, since equation (2) is calibrated based on the high-metallicity sources that have significant 24 μm emission, while most of our sources are metal-poor galaxies. We should also note that Calzetti et al. (2007) measure the SFR in individual H II regions in apertures within disks and subtract a "disk background," which could partly explain the deviations that we see from our analysis. These authors have also mentioned that the SFRs of low-metallicity galaxies would be underestimated by a factor of 2–4 depending on how metal-poor the galaxies are. This deviation from a linear correlation is likely due to the lower opacities for decreasing metal content (Walter et al. 2007). When we fit the filled circles on Figure 4, we find that $\log[\mathrm{SFR(IR)}] = 0.94\log[\mathrm{SFR}(1.4\ \mathrm{GHz})/3.98]$, which is consistent with the metallicity correction factor suggested by Calzetti et al. (2007). We should stress once more, however, that as Bell (2003) has noted, the good agreement between the IR and

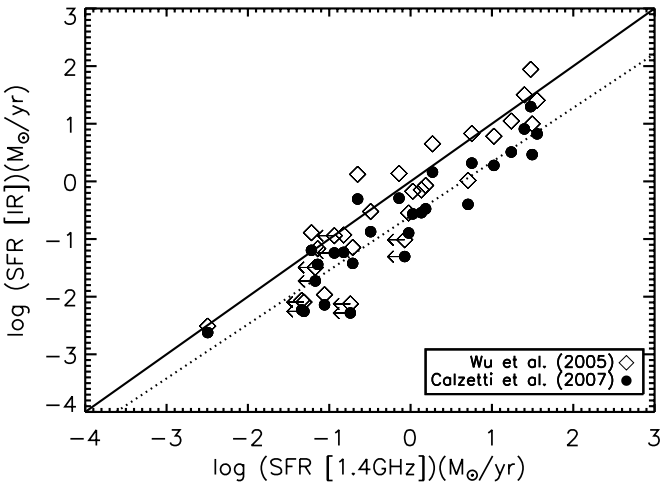

FIG. 4.—Plot of the SFR based on the 24 μm luminosity as a function of the corresponding SFR estimated from the 1.4 GHz radio continuum emission for each galaxy in our sample. The open diamonds indicate the SFRs calculated using the 24 μm fluxes following Wu et al. (2005; eq. [1]); the filled circles indicate those using eq. (2) from Calzetti et al. (2007). The solid line is the 1 : 1 proportionality line. The dotted line is a fit to the filled circles.

radio estimates of SFRs does not necessarily mean that these are the "true" SFRs for the dwarf galaxies that we study, but rather the competition of the lower dust content and suppressed synchrotron emission balances each other.

3.4. *The Two Extremes: I Zw 18 and SBS 0335−052E*

Despite this overall agreement between the IR/radio correlation in our dwarf sample and the corresponding values of normal galaxies, the two lowest metallicity galaxies in our sample, I Zw 18 and SBS 0335−052E, deviate markedly from the correlations and in opposite directions (see Fig. 3).[12] As these are the two most well studied BCDs, it is interesting to inspect the IR/radio properties of these two galaxies, and a comparison of their physical parameters can be found in Table 3.

As indicated by the *Spitzer* IRS spectrum of SBS 0335−052E (Houck et al. 2004b), the SED of the galaxy has an unusually flat mid-IR slope that peaks at ~28 μm. Hunt et al. (2005a) used DUSTY models (Ivezić et al. 1999) to fit its SED and found a $q_{\rm FIR}$ value of 2.0 for this galaxy, lower than the typical $q_{\rm FIR}$ of ~2.3 expected for late-type systems. These calculations are based on a 1.4 GHz continuum flux of ~0.46 mJy, which corresponds to the compact part (6″) of SBS 0335−052E (Dale et al. 2001; Hunt et al. 2004). Similarly, if we simply calculate the q ratio independent of any modeling work and only use the observable parameters, we find a $q_{70} = 2.1 \pm 0.1$ (assuming that the MIPS 70 μm flux density is 51.1 ± 4.8 mJy; Engelbracht et al. 2008). This is in good agreement with the $q_{70} = 2.16 \pm 0.17$ for the sources in the First Look Survey studied by Appleton et al. (2004).

However, when we examine the q_{24} for SBS 0335−052E, adopting a MIPS 24 μm flux of 66 mJy, we find a q_{24} ratio of 2.2 ± 0.1. We see a 2 σ excess in the q parameter compared with the mean q_{24} of 1.3 ± 0.4 in the dwarf sample. If this excess is real, it would be consistent with the unique shape of the SED of the galaxy, which suggests that the dust grain distribution is dominated by small grains with temperatures of ~150 K and a total dust mass of $\sim 10^3\ M_\odot$ (Houck et al. 2004b). Whether the large grains were never created or they were destroyed by shocks is unknown.

The elevated q_{24} ratio could also be due to the lack of synchrotron emission. Roussel et al. (2003, 2006) have shown their study of three starburst galaxies, all of which have $q_{\rm FIR}$ more than 3 σ higher than the mean $q_{\rm FIR}$, and categorized them to be nascent starbursts. SBS 0335−052E, however, could also be a candidate of this group. This is based partly on the high q_{24} value, as well as its low Hα luminosity as compared to the infrared or radio luminosities (see Table 3). Finally, Hunt et al. (2004) have shown the existence of free-free absorption in the radio spectrum of SBS 0335−052E, which is usually caused by young, dense, and heavily embedded clusters.[13]

I Zw 18, despite its similar metallicity to SBS 0335−052E [$12 + \log({\rm O/H}) = 7.17$ and 7.32, respectively], shows a rather different q ratio. It also has an IR luminosity of $L_{\rm IR} \sim 10^7\ L_\odot$, just 1% of the $L_{\rm IR}$ in SBS 0335−052E. In low-luminosity galaxies, radio emission is known to decrease faster than dust emission (Devereux & Eales 1989), and high IR/radio ratios have been observed in low-luminosity dwarf galaxies (Klein et al. 1984).

In I Zw 18, however, we find a rather low infrared-to-radio ratio. The q_{24} is found to be 0.5 ± 0.1, nearly 2 σ lower than the average value of our sample. At longer wavelengths, I Zw 18 is faint and no *IRAS* FIR data are available. However, as noted by Wu et al. (2007, see their Fig. 5), it has a very similar 5−38 μm continuum slope to the typical starburst galaxy NGC 7714 (Brandl et al. 2004). If we were to assume that this similarity extends to the FIR and scale down the *IRAS* 60 and 100 μm flux densities of NGC 7714 by a factor of 375 so that its corresponding 22 μm flux density matches that of I Zw 18, we would find its "equivalent" *IRAS* 60 and 100 μm flux density to be 29.8 and 32.8 mJy, respectively. This would result in $q_{\rm FIR}$ of 1.3 for the galaxy, which deviates from the average $q_{\rm FIR}$ ratio of 2.3 ± 0.2 calibrated by Condon (1992) by nearly 5 σ. If we were to use the MIPS 70 μm detection of 34 mJy for I Zw 18 (Engelbracht et al. 2008) and calculate its q ratio, we would find $q_{70} = 1.4$, again 5 σ away from the average q_{70} suggested by Appleton et al. (2004).

TABLE 3
COMPARISON OF SBS 0335−052E AND I ZW 18

Parameter	SBS 0335−052E	I Zw 18	Ratio[a]
$12 + \log({\rm O/H})$	7.32	7.17	1.4
D (Mpc)	58	18	3
R (pc)	560[b]	870[c]	~0.6
SFR ($M_\odot$ yr^{-1})	7×10^{-1}	5×10^{-2}	14
SN rate (yr^{-1})	6×10^{-3}	$2 \times 10 - 4$	30
$L_{\rm H\alpha}$ ($L_\odot$)	5.6×10^{7}[d]	1.6×10^{6}	35
$L_{24\ \mu{\rm m}}$($L_\odot$)	9×10^{8}	7×10^{6}	120
$L_{\rm IR}$ ($L_\odot$)	$\sim 4 \times 10^{9}$	$\sim 4 \times 10^{7}$	100
$L_{1.4\ {\rm GHz}}$ (W Hz^{-1})	2×10^{20}	8×10^{19}	2.5
$M(K_s)$ (mag)	−18.3	−16.1	~80[e]

[a] Ratio of the relative quantities in SBS 0335−052E to I Zw 18.
[b] This is the size of the six super star clusters in SBS 0335−052E, which has a size of 2″ (Thuan et al. 1997). At a distance of 58 Mpc, 1″ ~ 280 pc.
[c] This indicates the largest projected linear extent of the total star-forming regions in this galaxy (~10″; Hunt et al. 2005a). At a distance of 18 Mpc, 1″ ~ 87 pc.
[d] Flux in 1″ slit multiplied by a factor of 2 to correct for aperture effects.
[e] This is the approximate mass ratio of the two sources assuming that their mass scales with K-band luminosity and that both sources have the same M/L_{K_s} (see Bell & de Jong 2001).

[12] In Fig. 2 the "outlier" status of SBS 0335−052E does not appear as prominent as in Fig. 3, because its high 24 μm luminosity places it in a region of the plot where other sources with higher metallicity and higher luminosity are located.

[13] Note that if we could properly account for the self-absorption of the radio continuum, the intrinsic q ratio would decrease. However, the exact fraction for absorption is not known and more data at $\nu < 1.5$ GHz would be needed to determine that number.

A number of plausible scenarios were considered to explain this result, although none appears convincing. As discussed in Wu et al. (2008), because the optical depth of I Zw 18 is small, it could be that a significant fraction of the UV light has leaked out without being absorbed by the dust, thus resulting in a damped 24 μm emission. Alternatively, I Zw 18 may simply have an unusually high radio luminosity at 1.4 GHz. Could it be that I Zw 18 is observed at a special moment right after the explosion of a supernova event? Radio supernovae fade by more than a factor of 10 within $\sim$3 yr (Chevalier 1982). The radio continuum observations of I Zw 18 span a period of more than 5 yr (Hunt et al. 2005b; Cannon et al. 2005) but show no variation; thus, this is not likely.

The recent results by Murphy et al. (2006b) provide another possible scenario. These authors analyzed a sample of nearby spiral galaxies and found that systems with higher disk-averaged SFRs ($\Sigma_{\rm SFR}$) have usually experienced a recent episode of enhanced star formation. As a result they contain a higher fraction of young cosmic-ray electrons that have traveled only a few hundred parsecs from their acceleration sites in supernova remnants. This is perhaps the case for I Zw 18. However, other sources in our sample also have elevated $\Sigma_{\rm SFR}$ and show no radio excess. It could also be that the extremely low metal abundance of I Zw 18, 0.15 dex lower than that of SBS 0335$-$052E, is below a critical threshold. The newly formed stars in the unpolluted interstellar medium may produce, and subsequently heat, less dust than electrons, which are accelerated and contribute in the radio emission. We also note that the rate of SN in I Zw 18 is a factor of $\sim$30 lower than that in SBS 0335$-$052E (see Table 3) but its morphology is much more disturbed with filamentary structure and outflows (see Izotov & Thuan 2004). If we were to assume that both sources have similar mass-to-light ratios and estimate their mass from their *K*-band luminosities, we find that the mass of I Zw 18 is almost a factor of 80 less than that of SBS 0335$-$052E. Thus, the rate of SN normalized with mass in I Zw 18 would be $\sim$2.5 times that of SBS 0335$-$052E. Could it be that the disturbed morphology of I Zw 18, in addition to its low metal content is what created the conditions in the interstellar medium for this abnormally high radio flux? The question remains open.

4. CONCLUSIONS

We have studied the mid-IR– and FIR-to-radio correlation in a sample of dwarf star-forming galaxies spanning a metallicity range of $7.2 < 12 + \log({\rm O/H}) < 8.9$, using *Spitzer* IRS MIPS, as well as radio 1.4 GHz data obtained from the literature. The BCD sample appears to follow the same FIR/radio correlation as normal star-forming galaxies. The analysis based on mid-IR and radio data reveals a similar correlation, although the scatter is larger, probably due to an intrinsically higher variation in the 15$-$30 μm SEDs of dwarf galaxies. When comparing the q_{24} ratios with metallicity or effective dust temperature, we find no strong correlation, although there is a general trend of lower q ratios at lower metallicity for galaxies with $12 + \log({\rm O/H}) < 8.0$ and the correlation flattens out toward higher metallicity. In general the SFRs estimated from the radio 1.4 GHz continuum and the mid-IR data are in good agreement. Two extremely metal poor BCDs, I Zw 18 and SBS 0335$-$052E, appear to deviate from the average q_{24} by $\sim$2 σ, with one displaying a radio excess and the other an infrared excess.

The authors would like to thank P. Appleton and D. Calzetti for stimulating discussions. We would also like to thank G. Helou and L. K. Hunt, as well as an anonymous referee whose detailed comments and insightful suggestions have helped to improve this manuscript. This work is based in part on observations made with the *Spitzer Space Telescope*, which is operated by the Jet Propulsion Laboratory, California Institute of Technology, under NASA contract 1407. Support for this work was provided by NASA through contract 1257184 issued by JPL/Caltech. V. C. would like to acknowledge the partial support from EU ToK grant 39965.

REFERENCES

Allende Prieto, C., Lambert, D. L., & Asplund, M. 2001, ApJ, 556, L63
Aloisi, A., et al. 2007, ApJ, 667, L151
Appleton, P. N., et al. 2004, ApJS, 154, 147
Becker, R. H., White, R. L., & Helfand, D. J. 1995, ApJ, 450, 559
Bell, E. F. 2003, ApJ, 586, 794
Bell, E. F., & de Jong, R. S. 2001, ApJ, 550, 212
Bergvall, N., & Östlin, G. 2002, A&A, 390, 891
Boyle, B. J., Cornwell, T. J., Middelberg, E., Norris, R. P., Appleton, P. N., & Smail, I. 2007, MNRAS, 376, 1182
Brandl, B. R., et al. 2004, ApJS, 154, 188
———. 2006, ApJ, 653, 1129
Calzetti, D., et al. 2007, ApJ, 666, 870
Cannon, J. M., Walter, F., Skillman, E. D., & van Zee, L. 2005, ApJ, 621, L21
Chevalier, R. A. 1982, ApJ, 258, 790
Condon, J. J. 1992, ARA&A, 30, 575
Condon, J. J., Anderson, M. L., & Helou, G. 1991, ApJ, 376, 95
Condon, J. J., Cotton, W. D., Greisen, E. W., Yin, Q. F., Perley, R. A., Taylor, G. B., & Broderick, J. J. 1998, AJ, 115, 1693
Dale, D. A., Helou, G., Neugebauer, G., Soifer, B. T., Frayer, D. T., & Condon, J. J. 2001, AJ, 122, 1736
Dale, D. A., et al. 2006, ApJ, 646, 161
de Jong, T., Klein, U., Wielebinski, R., & Wunderlich, E. 1985, A&A, 147, L6
Devereux, N. A., & Eales, S. A. 1989, ApJ, 340, 708
Elbaz, D., Cesarsky, C. J., Chanial, P., Aussel, H., Franceschini, A., Fadda, D., & Chary, R. R. 2002, A&A, 384, 848
Engelbracht, C. W., Gordon, K. D., Rieke, G. H., Werner, M. W., Dale, D. A., & Latter, W. B. 2005, ApJ, 628, L29
Engelbracht, C. W., et al. 2008, ApJ, in press (arXiv: 0801.1700)
Garrett, M. A. 2002, A&A, 384, L19
Gruppioni, C., Pozzi, F., Zamorani, G., Ciliegi, P., Lari, C., Calabrese, E., La Franca, F., & Matute, I. 2003, MNRAS, 341, L1
Guseva, N. G., Izotov, Y. I., & Thuan, T. X. 2000, ApJ, 531, 776
Harwit, M., & Pacini, F. 1975, ApJ, 200, L127
Heckman, T. M., Robert, C., Leitherer, C., Garnett, D. R., & van der Rydt, F. 1998, ApJ, 503, 646
Helou, G., & Bicay, M. D. 1993, ApJ, 415, 93
Helou, G., Soifer, B. T., & Rowan-Robinson, M. 1985, ApJ, 298, L7
Hopkins, A. M., Schulte-Ladbeck, R. E., & Drozdovsky, I. O. 2002, AJ, 124, 862
Houck, J. R., et al. 2004a, ApJS, 154, 18
———. 2004b, ApJS, 154, 211
Hummel, E., Davies, R. D., Pedlar, A., Wolstencroft, R. D., & van der Hulst, J. M. 1988, A&A, 199, 91
Hunt, L. K., Bianchi, S., & Maiolino, R. 2005a, A&A, 434, 849
Hunt, L. K., Dyer, K. K., & Thuan, T. X. 2005b, A&A, 436, 837
Hunt, L. K., Dyer, K. K., Thuan, T. X., & Ulvestad, J. S. 2004, ApJ, 606, 853
Ivezić, Z., Nenkova, M., & Elitzur, M. 1999, User Manual for DUSTY (Lexington: Univ. Kentucky), http://www.pa.uky.edu/~moshe/dusty
Izotov, Y. I., & Thuan, T. X. 1998, ApJ, 500, 188
———. 1999, ApJ, 511, 639
———. 2004, ApJ, 616, 768
Jannuzi, B. T., & Dey, A. 1999, in ASP Conf. Ser. 191, Photometric Redshifts and the Detection of High Redshift Galaxies, ed. R. Weymann et al., (San Francisco: ASP), 111
Kennicutt, R. C., Jr. 1998, ARA&A, 36, 189
Kirshner, R. P., Oemler, A., Jr., Schechter, P. L., & Shectman, S. A. 1981, ApJ, 248, L57
Klein, U., Weiland, H., & Brinks, E. 1991, A&A, 246, 323
Klein, U., Wielebinski, R., & Thuan, T. X. 1984, A&A, 141, 241
Kobulnicky, H. A., & Johnson, K. E. 1999, ApJ, 527, 154
Kobulnicky, H. A., & Skillman, E. D. 1997, ApJ, 489, 636
Kunth, D., & Joubert, M. 1985, A&A, 142, 411

Leroy, A., Bolatto, A. D., Simon, J. D., & Blitz, L. 2005, ApJ, 625, 763
Miller, N. A., & Owen, F. N. 2001, AJ, 121, 1903
Moshir, M., et al. 1990, *IRAS* Faint Source Catalogue, Ver. 2.0 (Greenbelt: NASA)
Moustakas, J., & Kennicutt, R. C., Jr. 2006, ApJS, 164, 81
Murphy, E. J., et al. 2006a, ApJ, 638, 157
———. 2006b, ApJ, 651, L111
Popescu, C. C., & Hopp, U. 2000, A&AS, 142, 247
Rieke, G. H., et al. 2004, ApJS, 154, 25
Rosenberg, J. L., Ashby, M. L. N., Salzer, J. J., & Huang, J.-S. 2006, ApJ, 636, 742
Rosenberg, J. L., Wu, Y., Le Floc'h, E., Charmandaris, V., Ashby, M. L. N., Houck, J. R., Salzer, J. J., & Willner, S. P. 2008, ApJ, 674, 814
Roussel, H., Helou, G., Beck, R., Condon, J. J., Bosma, A., Matthews, K., & Jarrett, T. H. 2003, ApJ, 593, 733
Roussel, H., et al. 2006, ApJ, 646, 841
Sanders, D. B., Mazzarella, J. M., Kim, D.-C., Surace, J. A., & Soifer, B. T. 2003, AJ, 126, 1607
Sanders, D. B., et al. 2008, ApJS, in press (astro-ph/0701318)
Shi, F., Kong, X., Li, C., & Cheng, F. Z. 2005, A&A, 437, 849
Storchi-Bergmann, T., Calzetti, D., & Kinney, A. L. 1994, ApJ, 429, 572
Thuan, T. X., & Izotov, Y. I. 2005, ApJS, 161, 240
Thuan, T. X., Izotov, Y. I., & Lipovetsky, V. A. 1997, ApJ, 477, 661
van der Kruit, P. C. 1971, A&A, 15, 110
Walter, F., et al. 2007, ApJ, 661, 102
Werner, M. W., et al. 2004, ApJS, 154, 1
Wu, H., Cao, C., Hao, C.-N., Liu, F.-S., Wang, J.-L., Xia, X.-Y., Deng, Z.-G., & Young, C. K.-S. 2005, ApJ, 632, L79
Wu, Y., Bernard-Salas, J., Charmandaris, V., Lebouteiller, V., Hao, L., Brandl, B. R., & Houck, J. R. 2008, ApJ, 673, 193
Wu, Y., Charmandaris, V., Hao, L., Brandl, B. R., Bernard-Salas, J., Spoon, H. W. W., & Houck, J. R. 2006, ApJ, 639, 157
Wu, Y., et al. 2007, ApJ, 662, 952
Yun, M. S., Reddy, N. A., & Condon, J. J. 2001, ApJ, 554, 803